

RESEARCH

Open Access



Gallium nitrate inhibits multidrug-resistant *Acinetobacter baumannii* isolated from bloodstream infection by disrupting multiple iron-dependent metabolic processes

Zhuocheng Yao¹, Kaihang Yu^{1,2}, Changrui Qian¹, Beibei Zhou¹, Yishuai Lin¹, Xiaodong Zhang¹, Ying Zhang³, Tieli Zhou¹, Weiliang Zeng¹, Jianming Cao^{3*} and Yao Sun^{1*}

Abstract

Background *Acinetobacter baumannii* is a major pathogen in hospitals, causing a notable rise in bloodstream infections among inpatients. Its growing resistance to multiple drugs limits treatment options. This study aims to examine the antibacterial effects of gallium nitrate [Ga(NO₃)₃] against *A. baumannii* and elucidate the underlying molecular mechanism.

Methods 40 strains of *A. baumannii* with different antimicrobials susceptibility patterns were isolated from bloodstream infections. The in vitro antibacterial activity of Ga(NO₃)₃ was analyzed by micro-dilution method and time-kill assay. The influence of ferric chloride/hemin on the antibacterial efficacy of Ga(NO₃)₃ was investigated. Transcriptome sequencing was performed to elucidate the antibacterial mechanism of Ga(NO₃)₃. A mouse infection model was conducted to assess its in vivo performance.

Results Ga(NO₃)₃ exhibited a potent antibacterial effect in RPMI 1640 medium containing 10% human serum, with MICs ranging from 0.06 µg/mL to 0.125 µg/mL. The antibacterial activity of Ga(NO₃)₃ was found to be dose- and time-dependent. However, the antibacterial effect of Ga(NO₃)₃ was partially compromised in the presence of exogenous ferric chloride/hemin. Transcriptomics analysis revealed that Ga(NO₃)₃ exerted its antibacterial effect by up-regulating the expression of genes associated with siderophore biosynthesis and transport, while simultaneously disrupting multiple iron-dependent metabolic processes. Ga(NO₃)₃ treatment significantly reduced bacterial load in vivo using a neutropenic mouse thigh infection model.

Conclusion This study sheds light on the antibacterial mechanisms of Ga(NO₃)₃ against *A. baumannii*, suggesting its potential as a promising antibacterial drug for treating bloodstream infections caused by multidrug-resistant *A. baumannii*.

Keywords *Acinetobacter baumannii*, Gallium nitrate, Bloodstream infection, Siderophore, RNA-seq

*Correspondence:

Jianming Cao

wzcjming@163.com

Yao Sun

sunyaowzmu@163.com

Full list of author information is available at the end of the article



© The Author(s) 2025. **Open Access** This article is licensed under a Creative Commons Attribution-NonCommercial-NoDerivatives 4.0 International License, which permits any non-commercial use, sharing, distribution and reproduction in any medium or format, as long as you give appropriate credit to the original author(s) and the source, provide a link to the Creative Commons licence, and indicate if you modified the licensed material. You do not have permission under this licence to share adapted material derived from this article or parts of it. The images or other third party material in this article are included in the article's Creative Commons licence, unless indicated otherwise in a credit line to the material. If material is not included in the article's Creative Commons licence and your intended use is not permitted by statutory regulation or exceeds the permitted use, you will need to obtain permission directly from the copyright holder. To view a copy of this licence, visit <http://creativecommons.org/licenses/by-nc-nd/4.0/>.

Introduction

Acinetobacter baumannii is a significant hospital-acquired pathogen and has become the primary cause of bloodstream infections among inpatients, particularly those in intensive care unit (ICU) [1]. Its ability to acquire multidrug, extensively drug and even pandrug resistance severely limits the treatment options [2]. The mortality rate associated with *A. baumannii* bloodstream infection exceeds 50% [3, 4]. In China, the regimen based on sulbactam, colistin and tigecycline is recommended as the main treatment for carbapenem-resistant *A. baumannii* [5]. However, concerning reports of increasing resistance to the last-resort antimicrobials in *A. baumannii* have emerged [6]. Therefore, there is an urgent need to explore new therapeutic options to effectively treat bloodstream infections caused by multidrug-resistant *A. baumannii* (MDR-AB).

Blocking bacterial access to essential nutrients has become a promising anti-infection strategy. Iron, a critical nutrient for the survival of various bacteria, including *A. baumannii*, serves as a cofactor for multiple vital enzymes [7]. It plays a significant role in essential processes, such as DNA synthesis, electron transfer, and defense against reactive oxygen species [8]. A critical factor contributing to the success of *A. baumannii* as a nosocomial pathogen lies in its diverse mechanisms for acquiring iron, a vital but limited nutrient in vivo [7]. To date, six gene cluster associated with iron acquisition systems have been identified in *A. baumannii*. These includes two heme uptake gene clusters: heme uptake cluster I, which encodes a TonB dependent outer membrane receptor (TonB/ExbB/ExbD), periplasmic heme binding protein and an inner membrane ATP-binding cassette transporter; and heme uptake cluster II, which encodes a TonB dependent receptor, an extra cytoplasmic function (ECF) sigma factor, its cognate anti-sigma factor, and a putative heme oxygenase (*hemO*). Additionally, there are three siderophore clusters for acinetobactin (*bas/bau* gene cluster), baumannoferrin(s) (*bfn* gene cluster), and fimsbactin(s) (*fbbs* gene cluster), along with the ferrous uptake system Feo [9]. Given its critical role in bacterial physiology and pathogenicity, targeting iron uptake and metabolism has become attractive approach for developing new antimicrobials.

Gallium nitrate [$\text{Ga}(\text{NO}_3)_3$], an FDA-approved intravenous drug used to treat hypercalcemia associated with malignancy, has recently gained attention in antimicrobial research. Researches have revealed that metallic gallium acts as a “Trojan horse” by disrupting bacterial iron metabolism through gallium ions (Ga^{3+}), which share similarities with iron ions (Fe^{3+}) in terms of atomic radius and electron affinity [10]. Bacteria cannot differentiate gallium from iron, allowing Ga^{3+} to compete with Fe^{3+} at the iron binding site of enzymes. However, Ga^{3+} cannot

perform redox reactions like Fe^{3+} under physiological conditions, leading to the inhibition of essential physiological function [11]. $\text{Ga}(\text{NO}_3)_3$ has exhibited antibacterial activity against ESKAPE pathogens (*Enterococcus faecium*, *Staphylococcus aureus*, *Klebsiella pneumoniae*, *A. baumannii*, *Pseudomonas aeruginosa*, and *Enterobacter* species) [12]. Nonetheless, to our knowledge, there have been no reports of transcriptomics analysis to uncover the molecular mechanisms underlying antibacterial activity of Gallium against *A. baumannii*. Furthermore, in vivo studies of its antibacterial effect remain limited.

In this study, we demonstrated that $\text{Ga}(\text{NO}_3)_3$ had remarkable antibacterial effect against *A. baumannii*, both in a medium resembling human serum and in a neutropenic mouse thigh infection model. Our findings suggested that the antibacterial mechanism of gallium nitrate involved two main aspects: up-regulation of iron uptake and transport pathways and disrupting iron-dependent metabolisms of *A. baumannii*.

Results

The antibacterial activity of $\text{Ga}(\text{NO}_3)_3$ was influenced by different media

The antibacterial efficacy of $\text{Ga}(\text{NO}_3)_3$ was tested in four different media, of which MH broth represented an iron-rich environment, while the other three media provided iron-poor conditions. $\text{Ga}(\text{NO}_3)_3$ had no antibacterial activity in MH broth, with MICs exceeding 512 $\mu\text{g}/\text{mL}$. However, in M9CA medium, the MICs of $\text{Ga}(\text{NO}_3)_3$ against 40 *A. baumannii* strains ranged from 32 to 128 $\mu\text{g}/\text{mL}$. Similarly, in RPMI 1640 medium, the MICs of $\text{Ga}(\text{NO}_3)_3$ were observed to be between 32 and 64 $\mu\text{g}/\text{mL}$. The addition of 10% human serum to RPMI medium substantially enhanced the antibacterial activity of $\text{Ga}(\text{NO}_3)_3$, resulting in a remarkable reduction in MIC to the range of 0.0625 to 0.125 $\mu\text{g}/\text{mL}$. Notably, $\text{Ga}(\text{NO}_3)_3$ exhibited excellent antibacterial activity against both MDR strains and susceptible strains, indicating that its efficacy remained unaffected by the antimicrobial susceptibility patterns. The details of MICs in different media were listed in Table 1.

$\text{Ga}(\text{NO}_3)_3$ inhibits *A. baumannii* growth in a dose- and time-dependent manner

$\text{Ga}(\text{NO}_3)_3$ displayed a dose- and time-dependent inhibition of *A. baumannii* growth. The growth curves of *A. baumannii* BM-2333 under different concentrations of $\text{Ga}(\text{NO}_3)_3$ were shown in Fig. 1. The MIC value of BM-2333 in M9CA medium was determined to be 64 $\mu\text{g}/\text{mL}$. The growth of BM-2333 was effectively inhibited within 24 h when exposed to drug concentrations of 2 \times and 4 \times MIC. However, when treated with 1 \times MIC $\text{Ga}(\text{NO}_3)_3$, the growth inhibition was only observed in

Table 1 Susceptibility of gallium nitrate against *Acinetobacter baumannii* in different medium and iron uptake-related genes carried by *Acinetobacter baumannii*

Strains	MIC ($\mu\text{g/mL}$)				Gene		
	MH broth	M9CA	RPMI	RPMI + 10%HS	<i>basA</i>	<i>exbD</i>	<i>hemO</i>
BM-2333	>512	64	64	0.06	+	+	+
BM-4779	>512	64	64	0.125	+	+	+
BM-4825	>512	64	32	0.125	+	+	-
BM-4866	>512	64	64	0.125	+	+	+
BM-4870	>512	32	32	0.06	+	+	+
BM-4883	>512	64	64	-	+	+	+
BM-4995	>512	64	64	-	+	+	+
BM-5008	>512	32	32	-	+	+	+
BM-5021	>512	64	64	-	-	+	+
BM-5081	>512	32	64	-	+	+	+
BM-5119	>512	128	64	-	+	+	+
BM-5143	>512	64	64	-	+	+	+
BM-5166	>512	64	64	-	+	+	+
BM-5198	>512	64	64	-	+	-	+
BM-5235	>512	128	64	-	+	+	+
BM-5241	>512	32	64	-	+	+	-
BM-5265	>512	64	64	-	+	+	+
BM-5280	>512	64	64	-	+	+	+
BM-5314	>512	64	64	-	+	+	+
BM-5368	>512	64	64	-	+	+	+
BM-5395	>512	32	64	-	+	+	+
BM-5433	>512	64	32	-	+	+	+
BM-4795	>512	64	64	0.06	+	+	-
BM-4909	>512	32	64	≤ 0.06	+	+	-
BM-4915	>512	64	64	0.06	-	+	-
BM-4952	>512	32	64	0.06	+	+	-
BM-4953	>512	32	64	≤ 0.06	+	+	-
BM-4957	>512	64	32	-	+	+	-
BM-4994	>512	64	32	-	+	+	-
BM-5036	>512	64	64	-	+	+	+
BM-5057	>512	64	64	-	+	+	-
BM-5073	>512	32	64	-	+	-	+
BM-5179	>512	64	32	-	+	+	-
BM-5186	>512	64	32	-	+	+	-
BM-5211	>512	32	32	-	+	+	-
BM-5250	>512	64	64	-	+	+	-
BM-5260	>512	32	64	-	+	-	+
BM-5272	>512	64	32	-	+	+	-
BM-5318	>512	64	64	-	+	+	-
BM-5362	>512	32	32	-	+	+	-

Bold values are multidrug-resistant strains

All test strains can grow in RPMI + 10%HS without gallium nitrate. "-" represents "Not test" in the MICs

+: gene are positive

-: gene are negative,

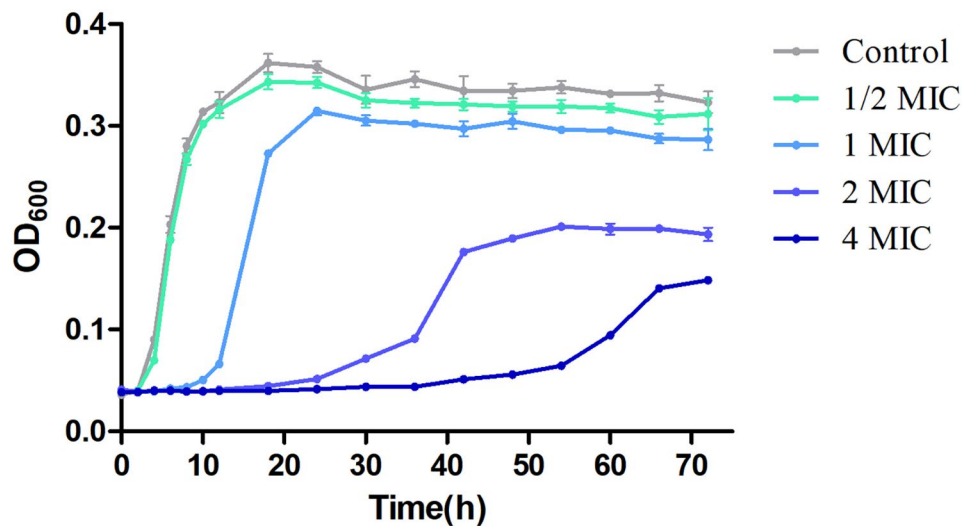


Fig. 1 The effect of $\text{Ga}(\text{NO}_3)_3$ on the growth of *A. baumannii* within 72 h

the early stage, and BM-2333 resumed growth at approximately 10 h. To further investigate the long-term effects, we extended the experiment to 72 h and monitored the growth curve. At 2× and 4× MIC concentration, the growth of strain BM-2333 eventually recovered over time. Interestingly, as the $\text{Ga}(\text{NO}_3)_3$ increased concentration, the maximum OD_{600} decreased, indicating that the growth potential of BM-2333 was hampered under higher $\text{Ga}(\text{NO}_3)_3$ concentrations.

Ferric chloride/hemin can weaken the antibacterial activity of $\text{Ga}(\text{NO}_3)_3$

The heatmaps illustrate the interaction between $\text{Ga}(\text{NO}_3)_3$ and iron chloride/hemin in Fig. 2. For BM-2333 and BM-4795, the results of the interaction between ferric chloride and $\text{Ga}(\text{NO}_3)_3$ exhibited similar patterns. As the concentration of ferric chloride increased, the antibacterial activity of $\text{Ga}(\text{NO}_3)_3$ weakened. However, at higher concentrations of $\text{Ga}(\text{NO}_3)_3$, it still displayed inhibitory effects on bacterial growth. This interaction was characterized as a competitive effect. However, the interaction between hemin and $\text{Ga}(\text{NO}_3)_3$ demonstrated distinct behavior. In the case of BM-2333, lower concentrations of hemin were able to restore the growth of strains, rendering it unresponsive to the inhibition effects of $\text{Ga}(\text{NO}_3)_3$ as its concentration increased. However, for BM-4795, the recovery of strain growth due to hemin was not remarkable, and could be suppressed by enhancing the concentration of $\text{Ga}(\text{NO}_3)_3$.

We further recorded the growth curve of BM-2333 and BM-4795 at the MICs (both were $0.0625 \mu\text{g}/\text{ml}$) (Fig. 3). In the case of BM-2333, the antibacterial activity of $\text{Ga}(\text{NO}_3)_3$ was found to weaken as the concentration of ferric chloride or hemin increases. Similarly, for BM-4795, the antibacterial activity of $\text{Ga}(\text{NO}_3)_3$

decreases with an increase in ferric chloride concentration. However unlike BM-2333, the growth of BM-4795 only showed partial restoration under high concentrations of hemin within 24 h.

Detection of iron-uptake genes

Due to the distinct hemin utilization abilities of BM-2333 and BM-4795, we conducted a comprehensive analysis of iron-uptake gene clusters. Among 40 *A. baumannii*, the positive rate for *exbD*, *hemO* and *basA* were found to be 92.5%, 57.5% and 95%, respectively. Notably, the positive rate of *hemO* of carbapenem-resistant *A. baumannii* (CRAB) was significantly higher than carbapenem-susceptible *A. baumannii* (CSAB) (90.9% vs. 16.7%, $p < 0.05$) (Table 1).

Transcriptomics analysis

According to RNA-Seq analysis, we identified a total of 1563 differentially expressed genes (DEGs) (Table S2). Among these, 755 genes were found to be up-regulated, while 808 genes were down-regulated in the $\text{Ga}(\text{NO}_3)_3$ treatment group compared to the control group (Fig. 4). The distribution of DEGs in various subcategories was visualized in Fig. S1, revealing their involvement in essential biological processes such as cellular process, metabolic process, cellular anatomical entity, intracellular, binding, catalytic activity and transporter activity. The GO classification enrichment of DEGs highlighted several significant GO Terms, including structural constituent of ribosome, structural molecule activity, ribosome, rRNA binding and oxidoreductase activity (Fig. 5).

Furthermore, KEGG enrichment analysis shed light on specific pathways influenced by $\text{Ga}(\text{NO}_3)_3$. Differentially up-regulated genes were found to be involved in ribosome and biosynthesis of siderophore group

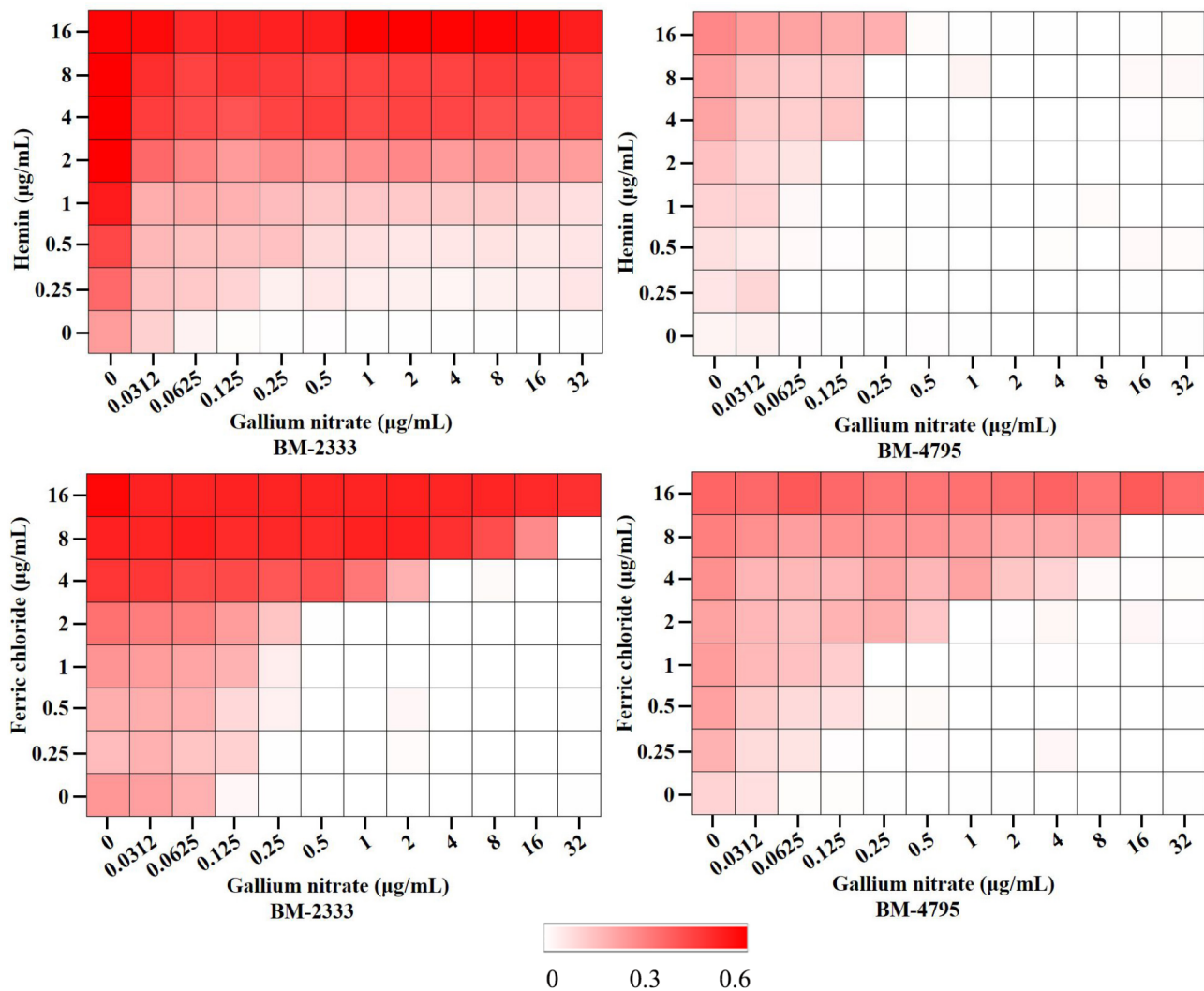


Fig. 2 The effect of exogenous iron chloride/heme on the antibacterial activity of $\text{Ga}(\text{NO}_3)_3$, x-axis: concentration of $\text{Ga}(\text{NO}_3)_3$, y-axis: concentration of iron chloride/heme. The growth of *A. baumannii* ranging from poor growth (white) to strong growth (red)

nonribosomal peptides pathway. Conversely, multiple pathways related to metabolism and degradation were differentially down-regulated (Fig. 6). As shown in Fig. 7, the expression levels of siderophore biosynthesis encoding gene *entA*, *entB*, *entC* and *entE*, and iron-siderophore transporters encoding gene *bauB*, *bauE* and *bauCD*, were significantly up-regulated. Concerning the oxidative phosphorylation pathway, the genes encoding NADH dehydrogenase and Succinate dehydrogenase were significantly down-regulated. Whereas, transcription of F-type ATPase was enhanced. In addition, the expressions of genes contributed to biofilm formation didn't demonstrate consistent trends, suggesting a complex regulatory mechanism at play (Fig. 7).

In vivo efficacy of $\text{Ga}(\text{NO}_3)_3$ in neutropenic mouse thigh infection model

The in vivo efficacy of $\text{Ga}(\text{NO}_3)_3$ was evaluated using a neutropenic mouse thigh infection model and the results were depicted in Fig. 8. Notably, the bacterial load in the thigh of the treatment group was significantly lower than the control group ($10^{7.00}$ CFU/g vs. $10^{5.39}$ CFU/g, $p < 0.05$), demonstrating the effectiveness of $\text{Ga}(\text{NO}_3)_3$ in reducing bacterial burden in the infected thighs of neutropenic mice.

Discussion

Bloodstream infections caused by multidrug-resistant *A. baumannii* (MDR-AB) have become a growing concern in hospitalized patients, particularly those in ICUs. However, the rise of MDR has severely restricted the availability of effective antimicrobials, posing a significant challenge in treating these infections [2]. It is worth

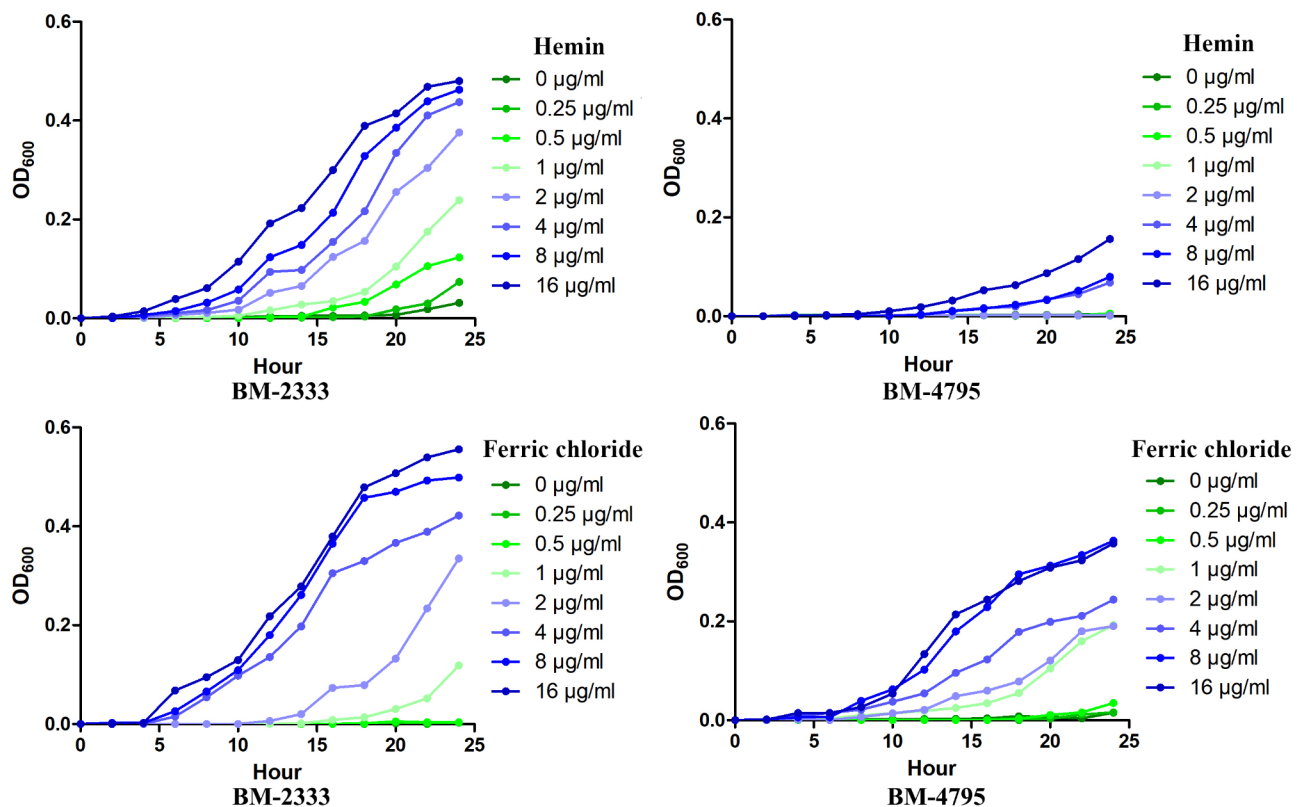


Fig. 3 Growth curves in *A. baumannii* under different concentrations of ferric chloride/hemin and MIC of $\text{Ga}(\text{NO}_3)_3$ interaction

noting that iron plays a crucial role in the growth and survival of *A. baumannii*, making it an attractive target for therapeutic intervention. Gallium, which is similar to iron, has the unique ability to disrupt proteins' function when it forms complexes with them. Hence, targeting iron metabolism could offer a promising approach for antibacterial therapy against MDR-AB infections.

The antibacterial activity of $\text{Ga}(\text{NO}_3)_3$ exhibited a dependence on the iron content of the medium in vitro, being more effective in iron-limiting conditions and chemically defined media, but less effective in iron-rich complex media. In mammalian hosts, Fe^{3+} is predominantly sequestered in iron-transport proteins, stored in ferritin, or bound in heme molecules, resulting in very low concentrations ($<10^{-18}$ M) of free Fe^{3+} [13]. Currently, there is lack of standard protocols or reference media for testing the sensitivity of $\text{Ga}(\text{NO}_3)_3$. MH broth is not suitable due to its high iron content. To address this, we followed the approach from the literature [14] and used an iron-deficient M9CA medium with constant chemical composition. Our data demonstrates that the MICs of $\text{Ga}(\text{NO}_3)_3$ against 40 *A. baumannii* strains ranged between 32 and 128 $\mu\text{g}/\text{mL}$ in M9CA medium. Remarkably, the MICs of $\text{Ga}(\text{NO}_3)_3$ were similar between MDR and sensitive groups, indicating that the antibacterial activity of $\text{Ga}(\text{NO}_3)_3$ was not affected by the

antimicrobials susceptibility patterns. Since there are few antimicrobials targeting iron metabolism in clinical practice, the mechanisms of action between $\text{Ga}(\text{NO}_3)_3$ and antimicrobials do not overlap. The growth curve demonstrated that $\text{Ga}(\text{NO}_3)_3$ inhibited *A. baumannii* growth in a dose- and time-dependent manner. Interestingly, despite concentration higher than the MIC, *A. baumannii* eventually recovered growth over time. However, the growth occurred at reduced maximum growth capacity as the concentration of $\text{Ga}(\text{NO}_3)_3$ increased. This observation points to a complex relationship between $\text{Ga}(\text{NO}_3)_3$ and bacterial growth, potentially involving adaptive responses to $\text{Ga}(\text{NO}_3)_3$ exposure.

In this study, the strains were isolated from bloodstream infections, prompting us to assess the antibacterial activity of $\text{Ga}(\text{NO}_3)_3$ in medium mimics human serum. Previous studies have proved that human serum created an iron-deficient environment for *A. baumannii* [15]. Therefore, it is crucial to investigate the practical significance of antibacterial effect of $\text{Ga}(\text{NO}_3)_3$ in human serum. To simulate the human blood environment and evaluate the MIC of $\text{Ga}(\text{NO}_3)_3$ at 18 h, we followed a method outlined in the literature [16]. Specifically, we used RPMI 1640 medium supplemented with 10% normal human serum. The results indicated a substantial reduction in the MIC of $\text{Ga}(\text{NO}_3)_3$ in the medium

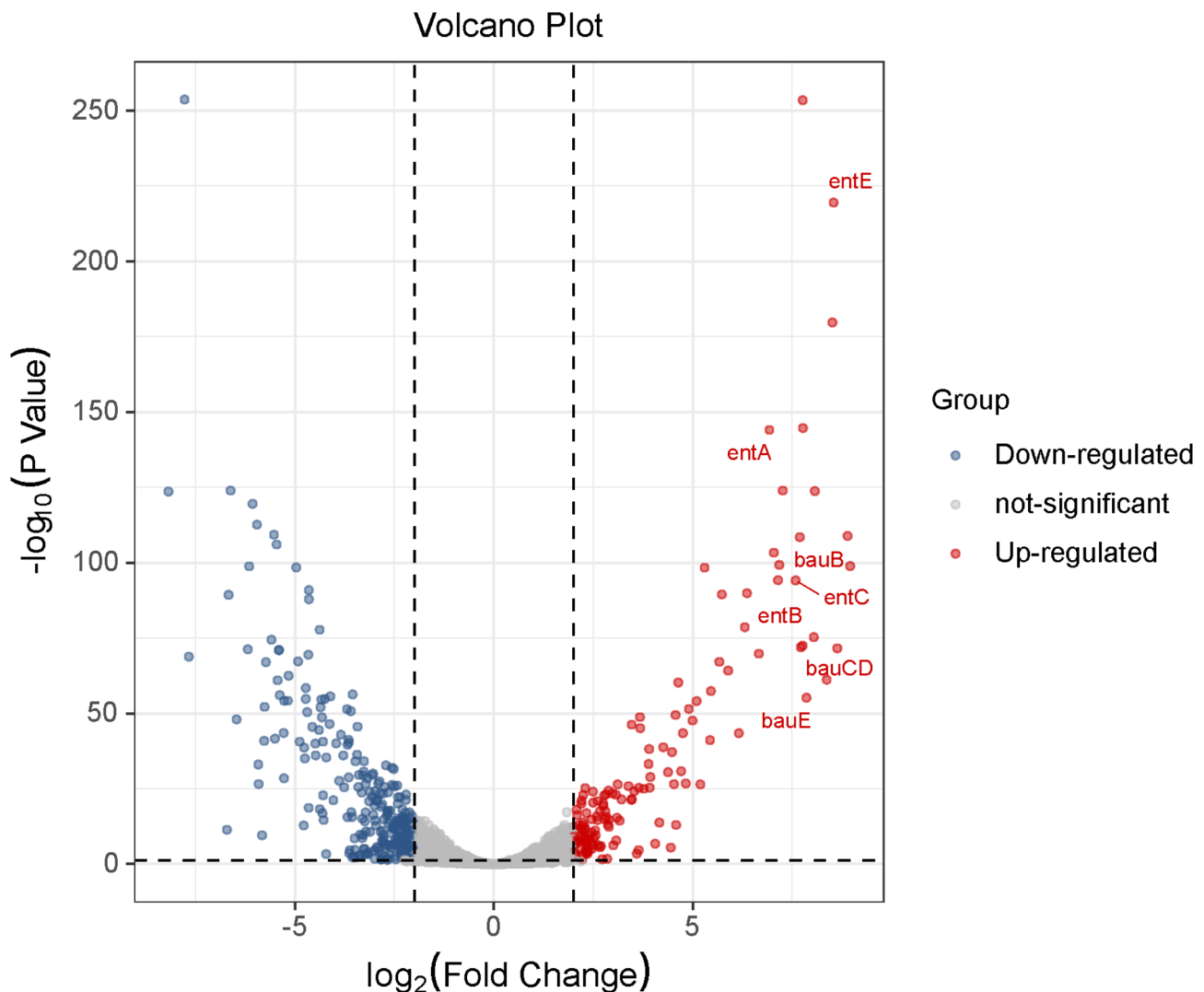


Fig. 4 The volcano plot of DEGs between control and experimental group, The X-axis represents the difference multiple value, and the Y-axis represents the significance value. Red represents up-regulated DEG, blue represents down-regulated DEG, and gray represents non-DEG

containing 10% serum compared to the pure RPMI 1640 medium, resulting in a range of 0.0625 to 0.125 $\mu\text{g}/\text{mL}$. Considering the peak plasma concentration of $\text{Ga}(\text{NO}_3)_3$ used to treat cancer-related hypercalcemia (300 mg/m^2 intravenously), approximately 28 μM or 7.2 $\mu\text{g}/\text{ml}$ [15]. This concentration was significantly higher than the MIC measured at 18 h. As $\text{Ga}(\text{NO}_3)_3$ exhibited dose-dependent inhibition of *A. baumannii* growth, we can infer that at the peak concentration, there will likely be a sustained antibacterial effect. Our findings support the notion that $\text{Ga}(\text{NO}_3)_3$ possesses potent antibacterial activity against *A. baumannii*, especially in an environment resembling human serum. The observed dose-dependent growth inhibition suggests that the peak plasma concentration of $\text{Ga}(\text{NO}_3)_3$ can potentially be effective in combating *A. baumannii* infections.

The antibacterial effect of $\text{Ga}(\text{NO}_3)_3$ was influenced by the environment, as supported by previous research [17]. We found that the presence of ferric chloride can competitively counteract the antibacterial activity of $\text{Ga}(\text{NO}_3)_3$. Similarly, heme, which is predominantly bound to hemoglobin in red blood cells and contains an iron ion in the center [18], can also weaken the antibacterial activity of $\text{Ga}(\text{NO}_3)_3$. However, the effect of hemin on $\text{Ga}(\text{NO}_3)_3$ varies among different strains, unlike the consistent effect observed with ferric chloride. *A. baumannii* had evolved a highly effective iron acquisition system to obtain iron from the iron-limited environment of the human host [19]. One such mechanism involves the release of siderophores, such as Acinetobactin, which acts as a high-affinity iron chelator to capture free or protein-bound iron, transporting it to the bacteria. Heme and heme-containing proteins constitute another

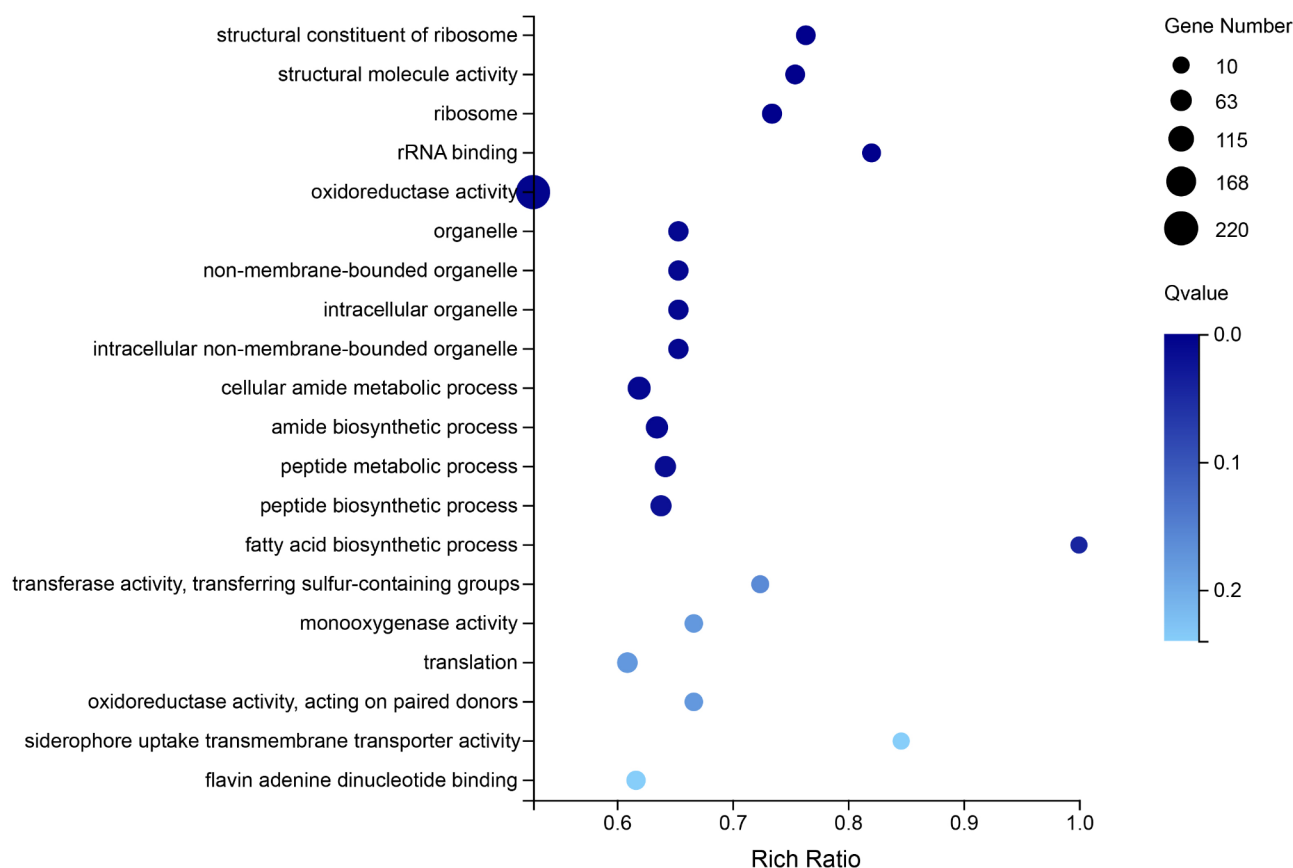


Fig. 5 GO analysis of DEGs. Bubble chart of GO enrichment of differentially expressed genes, The X axis is the enrichment ratio [the ratio of the number of genes annotated to an entry in the selected gene set to the total number of genes annotated to the entry in this species, the calculation formula: Rich Ratio = Term Candidate Gene Num / Term Gene Num], Y axis for GO Term, the size of the bubble represents the number of differential genes annotated to a GO Term, the color represents the enriched Q value, and the darker the color represents the smaller the Q value. Only differentially transcribed genes with absolute fold changes > 1 (\log_2 scale) and Q value < 0.05 were shown

significant source of iron in the body, accounting for approximately 70% of iron present. Antunes characterized two heme uptake clusters in *A. baumannii*, with the heme uptake cluster I being inherent, and heme uptake cluster II present in only two-thirds of the strains [20]. Upon capturing heme, the heme oxygenase of the bacteria degrades it, releasing free iron. Our data showed that the strains carrying only the heme uptake cluster I were less affected by exogenous heme. Only at high concentrations did exogenous hemin restore the growth of the strain. Conversely, strains carrying both heme uptake clusters were susceptible to the counteractive effects to low concentration of hemin on antibacterial effect of $\text{Ga}(\text{NO}_3)_3$. This finding aligned with a previous study suggesting that heme uptake cluster II played a major role in heme uptake [9]. Moreover, the heme uptake cluster II was crucial for optimal utilization of heme in *A. baumannii* hypervirulent strains [9]. The implications of our research are significant in clinical settings, as it helps identify situations where $\text{Ga}(\text{NO}_3)_3$ may not be suitable for use, such as in patients with hemolysis or conditions

involving excessive release of heme. Understanding the interplay between $\text{Ga}(\text{NO}_3)_3$ and the iron acquisition system in *A. baumannii* contributes to improved treatment strategies and more targeted antimicrobial use in specific patient populations.

To gain deeper insights into the antibacterial mechanism of $\text{Ga}(\text{NO}_3)_3$, transcriptome sequencing was conducted on *A. baumannii* after exposure to gallium nitrate. The enrichment analysis of GO and KEGG pathways revealed a significant enrichment of ribosome-related genes. The ribosome plays a crucial role in protein synthesis and function as one of the largest molecular machines in the cell [21]. Recent studies on *P. aeruginosa* have shown that the gallium ion targets the two subunits of RNA polymerase, RpoB and RpoC, which are gallium-binding proteins. This targeting of RNA polymerase by gallium suppresses RNA synthesis, resulting in reduced metabolic rates and energy utilization [14]. We found that the expression of ribosome-related genes was up-regulated in response to gallium nitrate treatment, indicating a defect in the protein translation process. To

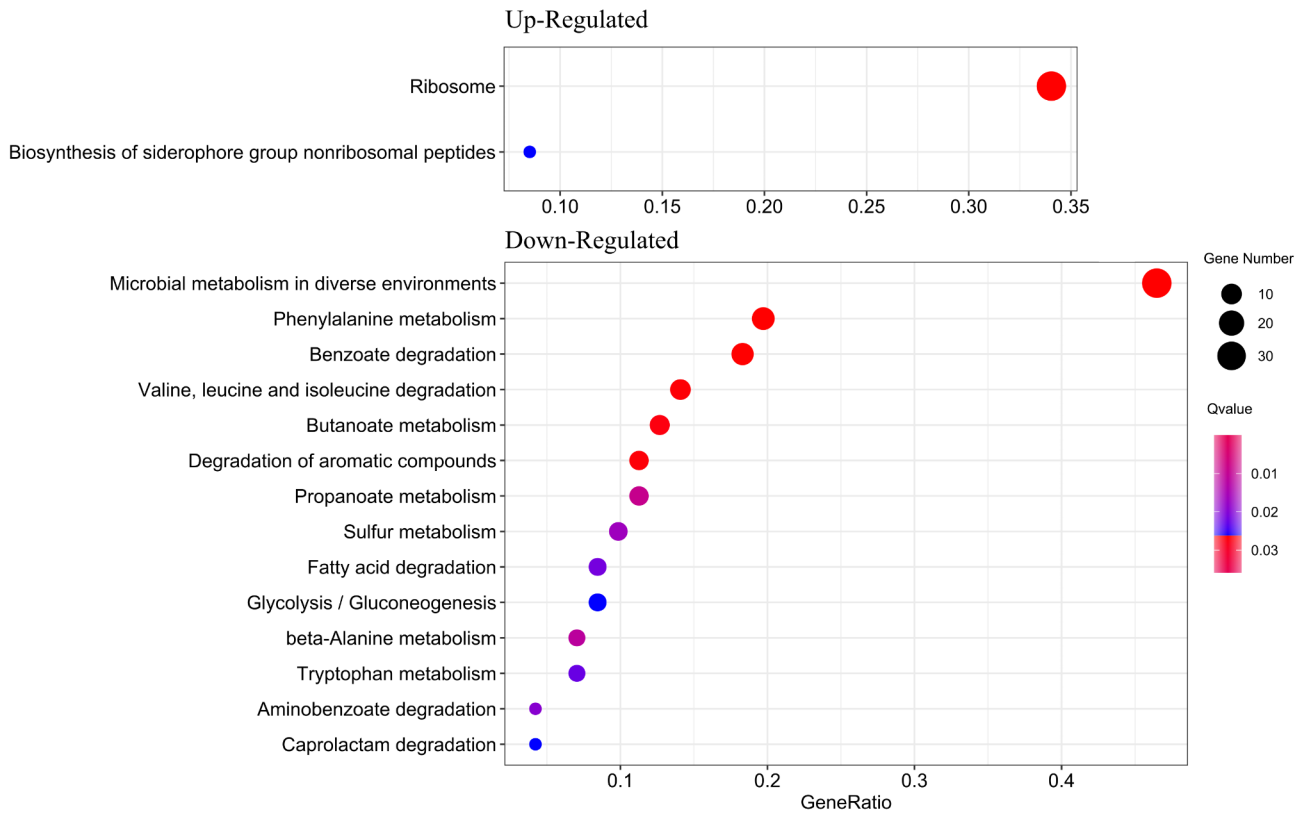


Fig. 6 Bubble chart of KEGG pathway enrichment of differentially expressed genes. The X-axis is the enrichment ratio, The Y-axis is KEGG Pathway, the size of the bubble represents the number of genes annotated to a KEGG Pathway, the color represents the enriched *p* value, and the darker the color, the smaller the *p* value. Only differentially transcribed genes with absolute fold changes > 1 (log₂ scale) and Q value < 0.05 were shown

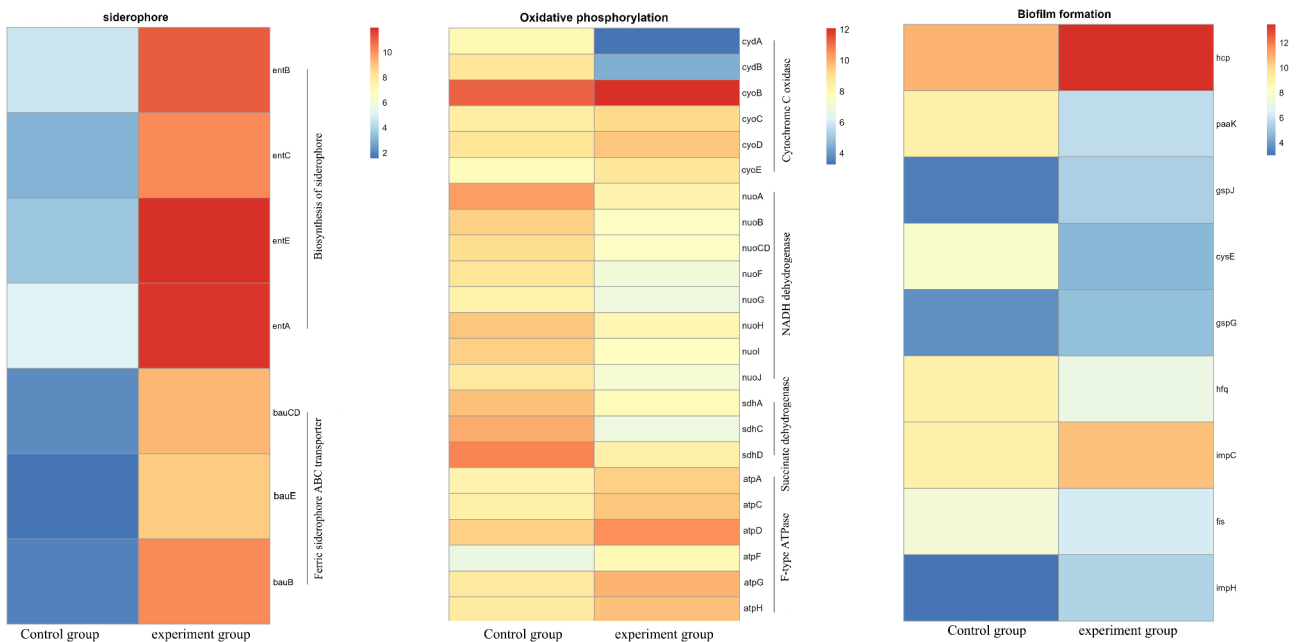


Fig. 7 Heatmap of differentially expressed genes involved in siderophore and transport, Oxidative phosphorylation and biofilm formation. The colors of the heatmap represent normalized gene expression levels (FPKM), ranging from blue (lower expression) to red (higher expression)

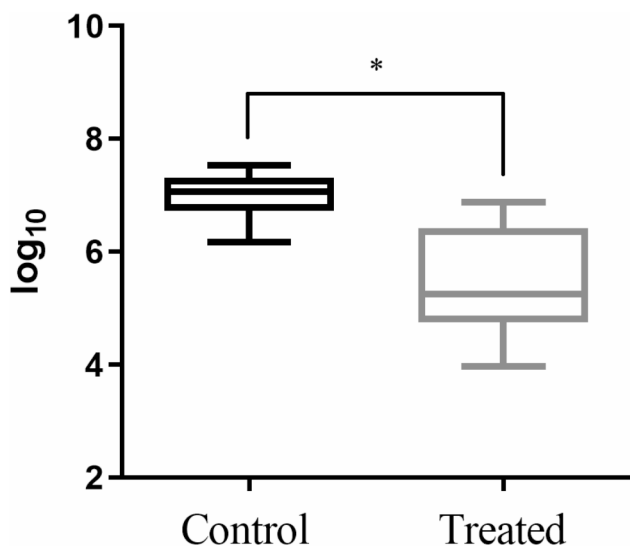


Fig. 8 Antibacterial effect of $\text{Ga}(\text{NO}_3)_3$ in the neutropenic mouse thigh infection model. * indicated $p < 0.05$

counteract iron-limitation, bacteria have developed high-affinity iron-uptake strategies, such as production of siderophore to bind iron and transport iron into the cell, utilization the heme iron by heme-binding proteins, and active iron transport mechanisms [12]. Our transcriptomics analysis revealed that differentially up-regulated genes associated with biosynthesis and transport of siderophore, which may be stimulated by the iron-deficient environment caused by $\text{Ga}(\text{NO}_3)_3$ treatment. Ga^{3+} can compete with Fe^{3+} for binding to enzymes that essential for various metabolic process [22]. Consequently, multiple pathways involved in metabolism and degradation were differentially down-regulated, potentially explaining the antibacterial mechanism of $\text{Ga}(\text{NO}_3)_3$. It is worth noting that $\text{Ga}(\text{NO}_3)_3$ has been found to inhibit the biofilm formation [23]. However, in this study the transcription of biofilm associated genes were heterogeneous, suggesting that the antibacterial effect of $\text{Ga}(\text{NO}_3)_3$ on biofilm formation may vary depending on different metabolic processes and warrants further investigation.

Previous studies had demonstrated the beneficial impact of $\text{Ga}(\text{NO}_3)_3$ on the survival of *Galleria mellonella* larvae infected with *A. baumannii* [15]. Moreover, recent finding had illustrated the effectiveness of $\text{Ga}(\text{NO}_3)_3$ in the treating chronic *P. aeruginosa* airway infections both in a mouse infection model and in a phase I clinical trial involving individuals with cystic fibrosis, and exhibited a lower propensity for resistance development compared to antimicrobials [24]. In this study, the neutropenic mouse thigh infection model verifies the antibacterial efficacy of $\text{Ga}(\text{NO}_3)_3$ on treating *A. baumannii* infection in vivo and demonstrated its potential of clinical application.

Conclusion

This study demonstrated the remarkable antibacterial efficacy of $\text{Ga}(\text{NO}_3)_3$ against multidrug-resistant *A. baumannii* both in vivo and in vitro. $\text{Ga}(\text{NO}_3)_3$ achieved its antibacterial effect by influencing the genes related to ribosome and siderophore, thereby disrupting multiple metabolism pathways of *A. baumannii*. Notably, the antibacterial effect was affected by the presence ferric chloride and hemin. Taken together, these findings point to the potential of $\text{Ga}(\text{NO}_3)_3$ as a novel therapeutic approach for combating bloodstream infections caused by multidrug-resistant *A. baumannii*, with a focus on targeting iron metabolism.

Materials and methods

Bacterial strains and culture conditions

The 40 *A. baumannii* strains used in this study and their antimicrobials susceptibility data were listed in Table S1 of supplemental material. These strains were isolated from patients with *A. baumannii* bloodstream infection at the First Affiliated Hospital of Wenzhou Medical University in 2018. The isolates were identified by the matrix-assisted laser desorption/ionization time of flight mass spectrometry (MALDI-TOF MS; bioMérieux, Lyons, France). 22 out of 40 strains were multidrug-resistance [25] and exhibited resistance to carbapenem.

Culture media used in this study were as follows: Mueller-Hinton (MH) broth, M9 minimal medium supplemented with 0.2% casein hydrolysate (hereby called M9CA) [14], and RPMI 1640 medium. To simulate human blood environment, when required, the media were supplemented with 10% human serum at appropriate concentrations. Human serum collected from 20 healthy donors was pooled, filtered, and inactivated (30 min, 56 °C) as described previously [26].

$\text{Ga}(\text{NO}_3)_3$ susceptibility testing

Antibacterial activity of $\text{Ga}(\text{NO}_3)_3$ was tested by microdilution method in four kinds of media, including MH broth, M9CA, RPMI 1640 medium and RPMI 1640 medium supplemented with 10% human serum (RPMI-HS). In brief, colonies were selected from a 24 h culture agar plate, suspended in 0.9% saline, and adjusted to a turbidity similar to that of a 0.5 McFarland standard. The saline suspension was diluted 1:200 in medium to obtain an inoculum density of approximately 5×10^5 CFU/mL. $\text{Ga}(\text{NO}_3)_3$ was 2-fold serially diluted in a 96-well microplate. The concentration range of $\text{Ga}(\text{NO}_3)_3$ was 0.03–32 $\mu\text{g}/\text{mL}$ for RPMI-HS, while for the other three media, it was 0.5–512 $\mu\text{g}/\text{mL}$. Growth control without drug and negative control (media only) were included in all experiments. A volume of 100 μL of this adjusted suspension was added to each well of the microtiter plates. The microtiter plates was read after 18 h of incubation in an

ambient-air incubator (except for RPMI 1640 medium, which was incubated in a 5% CO₂ incubator). Experiments were conducted in three biological replicates.

Time-kill assay

The impact of Ga(NO₃)₃ on the growth of *A. baumannii* BM-2333, a carbapenem resistant strain, was assessed according to a previously described method with slight modifications [12]. M9CA medium was employed to generate growth curve. Initially, the overnight bacterial cultures were 100-fold diluted and added to the sterile tubes containing different concentrations of Ga(NO₃)₃ (4×MIC, 2×MIC, 1×MIC, and 1/2×MIC), as well as tubes with no Ga(NO₃)₃ added for the growth control. The tubes were incubated with shaking at 37 °C. Samples were periodically taken from the culture for analysis. The absorbance at OD₆₀₀ was measured at 0, 2, 4, 6, 8, 10, 12, 18, 24, 30, 36, 42, 48, 54, 60, 66 and 72 h. Experiments were conducted in triplicate.

Exogenous ferric chloride/hemin addition assay

Carbapenem resistant strain BM-2333 and carbapenem susceptible strain BM-4795 were used in this experiment. The effect of exogenous ferric chloride/hemin on the antibacterial activity of Ga(NO₃)₃ was examined using the checkerboard assay. RPMI-HS was used for this test. Referring to the MICs of test isolates (0.0625 µg/mL), Ga(NO₃)₃ was 2-fold serially diluted along the x-axis (0–32 µg/mL), while ferric chloride/hemin was 2-fold serially diluted along the y-axis (0–16 µg/mL) to form a matrix, allowing each well to contain a combination of two drugs at varying concentrations. The single bacterial colony grown overnight was diluted to 0.5 McFarland turbidity in sterile saline, followed by 1:200 dilution in RPMI-HS. Subsequently, 100 µL of bacterial suspension was added to the corresponding well to achieve a final concentration of approximately 5 × 10⁵ CFU/mL. The 96-well plate was incubated in a 5% carbon dioxide incubator for 24 h and the growth situation (OD₆₀₀) was measured every 2 h. Relative growth of each well was defined as (OD₆₀₀ measured - OD_{600h}). Experiments were conducted in three biological replicates.

Genomic DNA extraction and PCR

Genomic DNA from the 40 experimental strains was extracted using Bioflux bacterial DNA extraction kit following the instructions of the manufacturer. Polymerase chain reaction (PCR) was used to detect iron-uptake gene clusters (The primer sequences are listed in Table S3), including heme-uptake gene cluster I (*exbD*), heme-uptake gene cluster II (*hemO*) and acinetobactin synthesis gene cluster (*basA*). The positive PCR product was sent to Shanghai Majorbio Bio-Pharm Technology Co. (Shanghai, China) for sequencing.

Genomic and transcriptomics analysis

Whole-genome sequencing (WGS) of *A. baumannii* BM-2333 was performed using long-read platform PacBio RS by the Beijing Genomics Institute (Wuhan, China). The plasmid and chromosome sequences of *A. baumannii* BM-2333 were used as the reference sequences for the subsequent RNA-seq read alignment and statistical analyses. *A. baumannii* BM-2333 cultured in M9CA medium with and without Ga(NO₃)₃ were defined as the experimental group and the control group, respectively. The cells were harvested at the exponential phase of growth for total RNAs extraction, following the Trizol/chloroform protocol, and then subjected to transcriptome sequencing analysis. The experimental group and the control group were carried out as three biological replicates. The RNA-seq data of six samples were filtered using SOAP nuke (v1.5.2). The RNA-seq reads were aligned to a reference coding gene set using Bowtie2 (v2.2.5), and the resulting alignments were used to calculate the expression levels of genes using RSEM (v1.2.12). Differential expression analysis was performed using the DESeq2 (v1.4.5) with Q value ≤ 0.05. To gain insight into the changes of phenotype, Gene Ontology (GO) and Kyoto Encyclopedia of Genes and Genomes (KEGG) enrichment analysis of annotated differential expressed genes was performed by Phyper based on Hypergeometric test. The significant levels of terms and pathways were corrected by applying a rigorous Q value threshold (Q value ≤ 0.05) by Bonferroni.

Neutropenic murine model

The neutropenic mouse thigh infection model was established to conduct in vivo studies [27]. Specific-pathogen-free (SPF) female ICR mice aged 5 to 6 weeks old (Charles river, Hangzhou, China), were used in this experiment. The mice were maintained in accordance with National Standards for Laboratory Animals of China (GB 14925–2010). To induce a neutropenia, we intraperitoneally injected cyclophosphamide (Yuanye Biotechnology Co., Ltd, Shanghai, China) at -4 day (150 mg/kg) and -1 day (100 mg/kg) prior to thigh infection. 100 µL suspension of exponentially growing bacterial at a concentration of 1.5 × 10⁷ CFU/mL were injected into each posterior thigh muscle. In vivo treatment studies commenced after 2 h following bacterial inoculation. Ga(NO₃)₃ was administered intraperitoneally at 300 mg/m²/24 h, based on the recommended dose [28]. The mice were euthanized by CO₂ inhalation after 24 h of therapy. Bacterial burden was quantified by CFU counts obtained from posterior thigh homogenates. Both the treatment group and the control group contained 6 mice (12 thigh infections).

Statistical analysis

Log₁₀-transformed CFU counts and log₂-transformed values of gene expression were used to calculate means and standard deviations for each dataset. Differences between means were assessed by the Student's t test. A *p*-value of <0.05 was considered statistically significant. All statistical calculations were conducted with SPSS v.22.0 software (SPSS Inc., Chicago, IL, USA).

Supplementary Information

The online version contains supplementary material available at <https://doi.org/10.1186/s12866-025-03950-4>.

Supplementary Material 1

Supplementary Material 2

Supplementary Material 3

Supplementary Material 4

Acknowledgements

Not applicable.

Author contributions

ZCY, KHY and BBZ carried out experiments. CRQ and YS performed the bioinformatics analysis. YSL, XDZ, and YZ analyzed the results and WLZ directed the drawing. ZCY wrote the manuscript. TLZ, JMC and YS designed the study and revised the manuscript. All authors reviewed and approved the final version of the manuscript.

Funding

This work was supported by: (i) the Zhejiang Province Natural Science Foundation of China (no. LY20H200004); (ii) the Major Projects of Wenzhou Science and Technology Bureau (no. ZY2019011); (iii) Key Laboratory of Clinical Laboratory Diagnosis and Translational Research of Zhejiang Province (no. 2022E10022).

Data availability

The genome data supporting the results of this article are deposited in the NCBI as BioProject PRJNA799658. The transcriptome data are available in the Gene Expression Omnibus (GEO) data repository under accession number GSE194255.

Declarations

Ethics approval and consent to participate

This study was approved by Ethics Committee in clinical research of the First Affiliated Hospital of Wenzhou Medical University (No. KY2022-R117), which waived the requirement for informed consent given the observational nature of this study, mainly focused on bacteria and involved no interventions with patients. Patient information was anonymized and de-identified during the entire process of data recording. All experiments were performed in compliance with the relevant laws and institutional guidelines in accordance with the ethical standards of the Declaration of Helsinki. Animal studies were approved by the Ethics Committee for Experimental Animals of the First Affiliated Hospital of Wenzhou Medical University (No. SYXK (Zhejiang) 2021-0017) and conducted in accordance with Wenzhou Laboratory Animal Welfare and ARRIVE guidelines.

Consent for publication

Not applicable.

Competing interests

The authors declare no competing interests.

Clinical trial number

Not applicable.

Author details

¹Department of Clinical Laboratory, Key Laboratory of Clinical Laboratory Diagnosis and Translational Research of Zhejiang Province, The First Affiliated Hospital of Wenzhou Medical University, Wenzhou 325000, Zhejiang Province, China

²Department of Pathology, the Second Affiliated Hospital, School of Medical, Zhejiang University, Hangzhou, Zhejiang Province, China

³School of Laboratory Medicine and Life Science, Wenzhou Medical University, Wenzhou 325000, Zhejiang Province, China

Received: 27 August 2023 / Accepted: 4 April 2025

Published online: 14 April 2025

References

1. Lin Y, Zhao D, Huang N, Liu S, Zheng J, Cao J, et al. Clinical impact of the type VI secretion system on clinical characteristics, virulence and prognosis of acinetobacter baumannii during bloodstream infection. *Microb Pathog*. 2023;182:106252.
2. Sun C, Yu Y, Hua X. Resistance mechanisms of tigecycline in acinetobacter baumannii. *Front Cell Infect Microbiol*. 2023;13:1141490.
3. Son HJ, Cho EB, Bae M, Lee SC, Sung H, Kim MN, et al. Clinical and microbiological analysis of risk factors for mortality in patients with carbapenem-resistant acinetobacter baumannii bacteremia. *Open Forum Infect Dis*. 2020;7(10):ofaa378.
4. Yu K, Zeng W, Xu Y, Liao W, Xu W, Zhou T, et al. Bloodstream infections caused by ST2 acinetobacter baumannii: risk factors, antibiotic regimens, and virulence over 6 years period in China. *Antimicrob Resist Infect Control*. 2021;10(1):16.
5. Chinese XDRCWG, Guan X, He L, Hu B, Hu J, Huang X, et al. Laboratory diagnosis, clinical management and infection control of the infections caused by extensively drug-resistant Gram-negative Bacilli: a Chinese consensus statement. *Clin Microbiol Infect*. 2016;22(Suppl 1):S15–25.
6. Jo J, Kwon KT, Ko KS. Multiple heteroresistance to tigecycline and colistin in acinetobacter baumannii isolates and its implications for combined antibiotic treatment. *J Biomed Sci*. 2023;30(1):37.
7. Artuso I, Poddar H, Evans BA, Visca P. Genomics of acinetobacter baumannii iron uptake. *Microb Genom*. 2023;9(8).
8. Cook-Libin S, Sykes EME, Kornelsen V, Kumar A. Iron acquisition mechanisms and their role in the virulence of acinetobacter baumannii. *Infect Immun*. 2022;90(10):e0022322.
9. Giardina BJ, Shahzad S, Huang W, Wilks A. Heme uptake and utilization by hypervirulent acinetobacter baumannii LAC-4 is dependent on a canonical heme oxygenase (abHemO). *Arch Biochem Biophys*. 2019;672:108066.
10. Guo Y, Li W, Li H, Xia W. Identification and characterization of a metalloprotein involved in gallium internalization in pseudomonas aeruginosa. *ACS Infect Dis*. 2019;5(10):1693–7.
11. Vinuesa V, Cruces R, Nonnoi F, McConnell MJ. Inhibition of LpxC increases the activity of iron chelators and gallium nitrate in multidrug-resistant acinetobacter baumannii. *Antibiot (Basel)*. 2021;10(5).
12. Hijazi S, Visaggio D, Pirolo M, Frangipani E, Bernstein L, Visca P. Antimicrobial activity of gallium compounds on ESKAPE pathogens. *Front Cell Infect Microbiol*. 2018;8:316.
13. Kelson AB, Carnevali M, Truong-Le V. Gallium-based anti-infectives: targeting microbial iron-uptake mechanisms. *Curr Opin Pharmacol*. 2013;13(5):707–16.
14. Wang Y, Han B, Xie Y, Wang H, Wang R, Xia W, et al. Combination of gallium(III) with acetate for combating antibiotic resistant pseudomonas aeruginosa. *Chem Sci*. 2019;10(24):6099–106.
15. Antunes LC, Imperi F, Minandri F, Visca P. In vitro and in vivo antimicrobial activities of gallium nitrate against multidrug-resistant acinetobacter baumannii. *Antimicrob Agents Chemother*. 2012;56(11):5961–70.
16. Arivett BA, Fiester SE, Ohneck EJ, Penwell WF, Kaufman CM, Relich RF, et al. Antimicrobial activity of gallium protoporphyrin IX against acinetobacter baumannii strains displaying different antibiotic resistance phenotypes. *Antimicrob Agents Chemother*. 2015;59(12):7657–65.
17. Li L, Chang H, Yong N, Li M, Hou Y, Rao W. Superior antibacterial activity of gallium based liquid metals due to Ga(3+) induced intracellular ROS generation. *J Mater Chem B*. 2021;9(1):85–93.
18. Gall T, Balla G, Balla J, Heme. Heme oxygenase, and endoplasmic reticulum stress—a new insight into the pathophysiology of vascular diseases. *Int J Mol Sci*. 2019;20(15).

19. Song WY, Kim HJ. Current biochemical understanding regarding the metabolism of acinetobactin, the major siderophore of the human pathogen *acinetobacter baumannii*, and outlook for discovery of novel anti-infectious agents based thereon. *Nat Prod Rep*. 2020;37(4):477–87.
20. Antunes LC, Imperi F, Towner KJ, Visca P. Genome-assisted identification of putative iron-utilization genes in *acinetobacter baumannii* and their distribution among a genotypically diverse collection of clinical isolates. *Res Microbiol*. 2011;162(3):279–84.
21. Paternoga H, Crowe-McAuliffe C, Bock LV, Koller TO, Morici M, Beckert B et al. Structural conservation of antibiotic interaction with ribosomes. *Nat Struct Mol Biol*. 2023;30(9):1380–92.
22. Song T, Zhao X, Shao Y, Guo M, Li C, Zhang W. Gallium(III) nitrate inhibits pathogenic *vibrio splendidus* vs by interfering with the iron uptake pathway. *J Microbiol Biotechnol*. 2019;29(6):973–83.
23. Xia W, Li N, Shan H, Lin Y, Yin F, Yu X, et al. Gallium porphyrin and gallium nitrate reduce the high vancomycin tolerance of MRSA biofilms by promoting extracellular DNA-dependent biofilm dispersion. *ACS Infect Dis*. 2021;7(8):2565–82.
24. Hijazi S, Visca P, Frangipani E, Gallium-Protoporphyrin IX. Inhibits *pseudomonas aeruginosa* growth by targeting cytochromes. *Front Cell Infect Microbiol*. 2017;7:12.
25. Magiorakos AP, Srinivasan A, Carey RB, Carmeli Y, Falagas ME, Giske CG, et al. Multidrug-resistant, extensively drug-resistant and pandrug-resistant bacteria: an international expert proposal for interim standard definitions for acquired resistance. *Clin Microbiol Infect*. 2012;18(3):268–81.
26. Rossato L, Arantes JP, Ribeiro SM, Simionatto S. Antibacterial activity of gallium nitrate against polymyxin-resistant *Klebsiella pneumoniae* strains. *Diagn Microbiol Infect Dis*. 2021;102(2):115569.
27. Zhou YF, Tao MT, Feng Y, Yang RS, Liao XP, Liu YH, et al. Increased activity of colistin in combination with amikacin against *Escherichia coli* co-producing NDM-5 and MCR-1. *J Antimicrob Chemother*. 2017;72(6):1723–30.
28. Coltery P, Keppler B, Madoulet C, Desoize B. Gallium in cancer treatment. *Crit Rev Oncol Hematol*. 2002;42(3):283–96.

Publisher's note

Springer Nature remains neutral with regard to jurisdictional claims in published maps and institutional affiliations.